Published in final edited form as:
Langmuir. 2006 February 14; 22(4): 1869–1874. doi:10.1021/la052187j.

Partitioning of Organic Compounds in Phases Imitating the Headgroup and Core Regions of Phospholipids Bilayers

Viera Lukacova, **Ming Peng**, **Roman Tandlich**, **Anne Hinderliter**, and **Stefan Balaz***
Department of Pharmaceutical Sciences, North Dakota State University, Fargo, ND 58105

Abstract

Solvation free energies of drugs, peptides, and other small molecules in the core and headgroup regions of phospholipid bilayers determine their conformations, accumulation, and transport properties. The transfer free energy includes the energy terms for the formation of a cavity for the solute, the interactions of the solute with phospholipids, electrostatic interactions of the solute with the membrane and dipole potentials, and entropy terms. The interaction energies with phospholipids can be estimated by correlating the partitioning in surrogate solvent systems and in the bilayer. As the headgroup surrogate, we use diacetylphosphatidylcholine (DAcPC), the acetylated headgroup of the most abundant mammalian phospholipid, phosphatidylcholine, which forms a homogeneous solution with acceptable viscosity, when mixed with water in ratios similar to those in the fully hydrated bilayer. The two-phase system of *n*-hexadecane (C16) as the core surrogate and hydrated DAcPC was used to monitor partitioning of sixteen nonionizable compounds. On the bilogarithmic scale, the C16/DAcPC partition coefficients correlate neither with those in the C16/water and 1-octanol/water systems, nor with their difference, which is frequently used as a parameter of hydrogen bonding for prediction of the bilayer location of the solutes. The C16/DAcPC system provides a satisfactory emulation of the solvation properties of the bilayer regions, as reflected in correct predictions of the bilayer location for those of the studied chemicals, for which this information is available.

Keywords

bilayer location; solvation energy in headgroup region; surrogate phase; diacetylphosphatidylcholine; transfer energy

Introduction

Interactions of chemicals with the headgroup and core regions of phospholipid bilayers play key roles in pharmacokinetics,[1–3] modification of membrane-anchored receptors,[4] anesthesia, 5 membrane protein folding6 and channel function,7 among other biologically relevant processes. Despite intense thermal motion,[8] the regions of (1) low headgroup density, (2) high headgroup density, (3) high tail density, and (4) low tail density can be discerned in a phospholipid bilayer.[9] Individual regions differ in shielding electrostatic charges, in the types of interactions, which the solute molecules experience, and in the free volume fractions that are important for diffusion of small molecules9,10 such as water,11 urea, formamide,[12] oxygen,[13] nitric oxide,[14] nonionized formic acid,[15] and others. A number of experimental techniques, mainly X-ray[16] and neutron diffraction,[17] NMR[18,19] and EPR[20] spectroscopy, and fluorescence quenching[21] have been used for characterization of the location of compounds in

CORRESPONDING AUTHOR FOOTNOTE: Stefan Balaz, Department of Pharmaceutical Sciences, Sudro Hall, Lab 8, North Dakota State University, Fargo, ND58105, phone 701-231-7749, fax 701-231-8333, e-mail stefan.balaz@ndsu.edu .

the phospholipid bilayer. For macromolecules, the atom-level details of the interactions with the bilayer regions are difficult to investigate because of the size of the molecules.

Partitioning equilibria of solutes in bilayer regions result from the interplay of several factors that include the interactions of solutes with phospholipids, the energy to create the cavities for solute molecules, electrostatic interactions with the membrane and dipole potentials,[22] and entropic consequences of partitioning in individual regions.[23–25] Estimates for the first factor have traditionally been obtained using organic solvents as surrogates of the bilayer or its regions. The partition coefficients P in two solvent systems that are capable of similar interactions with the studied compounds are related according to the Collander equation:[26]

$$P_2 = \alpha \times P_1^{\beta} \quad (1).$$

The parameters α and β are obtained by the fit to the experimental data. The approach is widely used in the design of bioactive compounds,[27] computational chemistry,[28] protein folding,[29] and other areas.[30]

After early experiments with loosely defined oils[31–35] and other organic phases,[26,36] 1-octanol became a widely used solvent.[37] The authors and many followers in the area of quantitative structure-activity relationships (QSARs) in the design of bioactive compounds intuitively considered hydrated 1-octanol to be the hydrocarbon core surrogate, despite its comparatively high equilibrium water content that at room temperature equals 2.18 mol/l.[38] This fact can be reconciled with the aforementioned view using the observation of the water transport in the hydrocarbon core,[11] although the core seems to be almost dry under equilibrium conditions.[39,40] Contrary to the core surrogate hypothesis, studies in peptide binding to liposomes[41] and in transport through black lipid membranes[42] assume that 1-octanol mimics the headgroup region of the bilayer. Interestingly, both views can be correct: X-ray diffraction analyses,[43] spectroscopic investigation,[44] and molecular dynamics simulations[45,46] of the structure of liquid, water-saturated 1-octanol revealed fluctuating polar and nonpolar regions including inverted micellar aggregates that could imitate both cores and hydrated headgroup regions. Consequently, while 1-octanol seems to be a good bilayer surrogate for estimation of the overall bilayer partitioning, its amphiphilic character may complicate its use for characterization of solvation in individual regions.

As the criteria for selection of a proper surrogate, early studies used partitioning into cells and transport through biological films that are affected by protein binding and other bilayer-unrelated factors. These problems are avoided when using phospholipid liposomes that are more suitable for evaluation of the surrogate phases. Liposome partitioning is affected by the temperature, which should be well above the gel-fluid phase transition temperature,[47] fluidity,[48] phospholipid surface density,[49] and other mutually related factors.[50] Ideally, all data for a comparison should be measured under identical conditions imitating the studied biological system. The partition coefficients of chemicals in liposomes and in the 1-octanol/water system were correlated, on a bilogarithmic scale, with separate dependencies for neutral, positively charged, and negatively charged molecules.[51] The relationships break down even for homologous series exhibiting different preferred bilayer locales for individual members.[52] If diverse chemicals are considered, the relationship seems to hold, with a wider scatter and within certain size and lipophilicity limits,[53] for neutral molecules[54] but not for charged molecules.[55,56] A careful analysis of the data measured in a single laboratory showed that even for neutral chemicals, different lines can be discerned for polar and nonpolar compounds.[57] More variation can be expected for compounds with different H-bond donor groups.

The studies with black lipid membranes showed that the selectivity of the bilayer to the partitioning of the H-bonding groups lies somewhere between those of 1-octanol and pure hydrocarbon,[58] but is significantly closer to that of the latter.[59,60] Additional support for the use of hydrocarbons as the core surrogates[61,62] comes from the experimental observation of similar molecular packing of the fatty acyl methylene and methyl groups in region 4 of the bilayer and in bulk liquid alkanes.[63]

Four solvents, 1-octanol, propyleneglycol dipelargonate, chloroform, and alkane, were used to model the amphiprotic, H-bond acceptor, H-bond donor, and hydrophobic properties of membranes:, respectively.[64] In all mentioned two-phase systems, the bilayer is mimicked by an organic solvent and the difference in solvation free energies is measured against water. The ethylene glycol/heptane system[65] represents a rare attempt to imitate separately the headgroups and the core regions of the bilayer. None of the solvents used so far emulates the charged functional groups of phospholipids.

A straightforward approach to include all functional groups of phospholipids into the surrogate system is to split the phospholipid molecules into the headgroups and the alkanes. We have found that the phosphatidylcholine (PC) headgroup with truncated fatty acid chains, diacetylphosphatidylcholine (DAcPC), when dissolved in water in a molar ratio of 1:14 (1.96 M) corresponding to the hydration shell of the PC headgroup in the gel-liquid bilayer not far above the transition temperature,[66,67] forms a homogeneous and only slightly viscous solution. The hydrated DAcPC has the same composition as the PC headgroup region. The methyl groups in the DAcPC acetyls imitate the few methylenes of fatty acids that fluctuate at the level of carbonyls in a PC bilayer and can be considered a part of the headgroup region.8 Alkanes seem to be a good surrogate for the core.[59–63] In contact, hydrated DAcPC and *n*-hexadecane (C16) exhibit minimal mutual solubilities. In this study, partitioning of a set of compounds between hydrated DAcPC and C16 is measured and compared with partitioning in other solvent systems, with a special emphasis on the prediction of the preferred bilayer location. Isotropic two-phase systems can be used to estimate, via the Collander equation 1, the interactions with the surrounding phospholipids. The solvent systems cannot capture the effects of the cavity formation energy, electric fields, and entropy in the bilayer. Relative contributions of the four factors to the bilayer partitioning vary depending on the solute properties. The cavity formation energy can probably be parametrized using the molecular mass, molecular volume, or the cross-sectional area of the solutes, although the choice of the area (minimal, maximal, or expected in the dense bilayer regions 2–3) may not always be straightforward.[22,68–71] The membrane and dipole potential have the largest impact on the charged molecules. The entropic anomalies were observed for large aromatic molecules and only affect the distribution between the high-density and low-density tail regions 3 and 4, respectively.[23–25] We hypothesize that, for neutral molecules of similar sizes, the C16/DAcPC transfer free energies will correlate with similar quantities for the transfer from the core to the headgroup region better than those in other solvent systems because of the close match in chemical composition of the phases.

Experimental Section

Chemicals

DAcPC was obtained from Euticals (Prime European Therapeuticals S.p.A, Lodi, Italy). All studied solutes and C16 were purchased from Sigma-Aldrich (St. Louis, MO).

Mutual Phase Dissolution

The DAcPC phase (2.5 ml) and 8.5 ml of C16 were incubated on a rotary shaker at 25°C. The phases were separated and analyzed at appropriate times up to 48 h. DAcPC from 2 ml of the C16 phase was extracted to 1.2 ml of water. Water was evaporated under the stream of nitrogen

and the amount of DAcPC was determined by the modified Bartlett's phosphate assay.[72] The DAcPC phase (0.8 ml) was transferred into a 2.0 ml clear glass vial and allowed to equilibrate with the gas phase for 15 minutes. The headspace was then sampled for hexadecane using a 65 μm Carbowax/divinylbenzene SPME fiber (Supelco, Bellefonte CA). The extraction was performed under static conditions with 10 min exposure. Analysis was done using GC/MS/MS-Ion Trap (Varian 3800/Saturn 2000; Varian, Inc.; Palo Alto, CA).

Thermal Behavior of Hydrated DAcPC

The hydrated DAcPC phase (1.96 M) was examined for phase transitions by differential scanning calorimetry (Microcal, LLC, Northampton, MA). The phase was analyzed in cooling regimen in range 80°C to 5°C with a scanning rate of 15°C/hr. No transitions were detected; therefore, hydrated DAcPC is regarded as an isotropic phase.

C16/DAcPC Partitioning

For partitioning measurements, the two phases were mutually saturated by the 8-h contact, although less than 1 h is sufficient to obtain the equilibrium. After separation of the phases, the measured compound was dissolved in the C16 phase and the solution was surfaced on the DAcPC phase. For 2,6-dimethoxyphenol and 2,3-diaminonaphthtalene, the partitioning from hydrated DAcPC to C16 was also monitored. The volume ratio of the two phases was estimated on the basis of the structure of the compound and preliminary experiments so that the expected change in the drug concentration in the C16 phase was at least 5% but no more than 95%. For each compound, eight samples were set up at the beginning of the experiment and incubated at 25°C on an orbital shaker. The samples were withdrawn from the shaker at the times varying from 0 to 5 h, and the amount of the compound left in the C16 phase was determined by UV spectroscopy (UV-1601; Shimadzu Scientific Instruments, Columbia, MD). The experiments were carried out in test tubes (16 × 100 mm, volume 11 ml) with screw caps and PTFE septa to prevent evaporation. For most compounds, the equilibrium was reached in less than 2 h. Along with each sample, a control containing only the compound dissolved in the C16 phase was processed to account for possible evaporation of the compound.

Partitioning Data Analysis

For all measured compounds, the equilibrium was reached within the duration of the experiment and so the equilibrium data analysis was used to determine the partitioning of the compound (Figure 1). The partition coefficient $P_{C16/DAcPC}$ was calculated directly from the equilibrium concentrations c:

$$P_{C16/DAcPC} = \frac{c_{C16}(eq)V_{DAcPC}}{[c_{C16}(0) - c_{C16}(eq)]\,V_{C16} - Hc_{C16}(eq)V_{air}} \quad (2).$$

Here, V are the volumes, the subscripts denote individual phases, and the terms in the brackets indicate the time t = 0 and the equilibrium, respectively. To correct for evaporation, the dimensionless Henry constant, H, was calculated using the control samples:

$$H = \frac{[c_{C16}(0) - c_{C16}(eq)]\,V_{C16}}{c_{C16}(eq)V_{air}} \quad (3).$$

To confirm that the partitioning equilibrium has been reached, the C16/DAcPC partition coefficients were also calculated by fitting the time-dependent decrease of the drug concentrations in the hexadecane phase upon partitioning into the DAcPC phase. For this purpose, a scheme similar to that in Figure 1 was used, with the two equilibrium constants

replaced by the respective pairs of the rate constants. The linear differential equations describing the scheme were solved for the full scenario, as well as for the absent evaporation and for the transfer being much faster than evaporation. The fits[73] of the kinetic data provided results similar to those of the equilibrium analysis.

Results and Discussion

The two-phase C16/DAcPC system was characterized before its use for partitioning experiments. At 25°C, the equilibrium concentration of C16 in the DAcPC phase was equal to 130 ng/ml (0.574 μM), while that of DAcPC in the C16 phase was below the detection limit of the used method, i.e., less than 1 ng/ml (3 nM). The low equilibrium concentrations of DAcPC and C16 in the opposite phases are expected to have a negligible influence on the partitioning of the studied compounds, whose concentrations are mostly close to the millimolar range for analytical reasons. The hydrated DAcPC phase (1.96 M) did not exhibit phase transitions when examined by differential scanning calorimetry and is regarded as an isotropic phase.

For partitioning measurements, the DAcPC and C16 phases were mutually saturated. The measured compounds (Table 1) were dissolved in C16, and the solution was surfaced on the DAcPC phase in closed 11-mL test tubes to prevent evaporation. Along with each sample, a control containing only the compound dissolved in the C16 phase was processed to monitor possible evaporation of the compound. The kinetic and equilibrium data were processed according to the scheme given in Figure 1. For two compounds, the partitioning was measured in both directions, from the C16 phase to the DAcPC phase as well as from the DAcPC phase to the C16 phase, with a reasonable agreement between the partition coefficients. The obtained $\log P_{C16/DAcPC}$ values for the C16-to-DAcPC partitioning and DAcPC-to-C16 partitioning were −1.054 ± 0.025 and −0.996 ± 0.010 for 2,6-dimethoxyphenol and −1.694 ± 0.073 and −1.691 ± 0.019 for 2,3-diaminonaphthalene, respectively. The kinetics of partitioning and evaporation for one of the studied compounds, pyridine (**10**, Table 1), is shown in Figure 2. The measured partition coefficients *P* are summarized in Table 1, along with the *P* values for the C16/water system and 1-octanol/water system (C16/W and O/W, respectively), which are often used as surrogate phases, and the comparison with the studied system is of interest.

The C16/DAcPC partition coefficients *P* significantly differ from those in the C16/W and O/W systems for all compounds except for compounds **2** and **3**, indicating different solvations of the chemicals in these systems. The dependencies of the *P* values, on the bilogarithmic scale, are shown in Figure 3. Also included are the values of the difference $\log P_{C16/W} - \log P_{O/W}$ that are formally equal to the $\log P_{C16/O}$ values (1-octanol is frequently assumed to imitate solvation in the headgroup region[41,42]). The correlations are far from perfect. The characteristics of the linear fits for $\log P_{C16/W}$, $\log P_{O/W}$, and $\log P_{C16/O}$, respectively, are: slopes of 1.091, 0.665, and 0.462; intercepts of 0.406, 2.011, and −1.606; standard deviations of 1.347, 1.351, and 0.805; and squared correlation coefficients, equal to the percentage of explained variance, of 0.817, 0.614, and 0.606. Obviously, $\log P_{C16/DAcPC}$ is coding unique solvation information that cannot be obtained using the two common two-phase systems. Is this information relevant for the bilayer partitioning?

The C16/DAcPC partition coefficients were used to estimate the equilibrium distribution of compounds in the fluid PC bilayers on an amount basis (Table 1), using the headgroups/core volume ratio 2:3 as in the dimyristoylphosphatidylcholine bilayer.[67] The estimated distribution agrees well with the experimental data, although the results for solutes **2**, **6**, and **16** deserve some discussion. For benzene (**2** in Table 1), both the headgroups and core have been reported as the preferred locale in separate studies[75,76] and our treatment favors the core, in accord with the MD simulations.[45] 9-Anthracenemethanol (**6** in Table 1) anchors at the interface, with the

hydroxy group interacting with the headgroups and the rest of the molecule solvated in the core.[21] For bisphenol A (**16** in Table 1), the NMR data indicate that practically the entire molecule interacts with the headgroup region and only the two methyl groups are in contact with the first two methylenes of the fatty acid chains. Since the first two to three methylenes of the sn-2 fatty acid fluctuate at the level of the carbonyl groups of the fatty acids,[8] bisphenol A can be considered as solvated in the headgroup region, in accord with the C16/DAcPC prediction.

The difference $\log P_{C16/W} - \log P_{O/W}$ (formally equal to $\log P_{C16/O}$) is frequently considered an indicator of the hydrogen-bonding ability[65,79–81] and, consequently, as a parameter characterizing the preferential location of the solutes in the bilayer. The fraction of compounds present in the core as a function of $\log P_{C16/O}$ is plotted in Figure 4. As summarized in Table 1, experiments show that compounds **1–4** partition into the core, compound **6** sticks to the interface, and compounds **10**, **12**, **15**, and **16** interact preferentially with the headgroups. To connect the compounds with a known locale in the headgroups or in the core (except compound **6** in Table 1), the data were fitted[73] with the Boltzmann sigmoidal function:

$$F_{core} = 100 - \frac{100}{1+\exp[(\log P_{C16/W} - \log P_{O/W} + 0.776)/0.215]} \quad (4).$$

Standard deviations of the optimized parameters are less than 20% of the parameter values and the squared correlation coefficient is $r^2 = 0.992$. All compounds were included except the outliers **5–9** (Table 1).

The compounds with the $\log P_{C16/O}$ values larger than −0.5 are expected to partition to the core ($F_{core} > 80\%$) and those with the $\log P_{C16/O}$ values below −1.0 or so are anticipated to associate with the headgroup region ($F_{core} < 20\%$). The $\log P_{C16/O}$ values between −1.0 and −0.5 indicate that the compound has no clear preference for the core or the headgroups and can partition in both phases and/or at the interface. The exact limits depend on the phospholipid and the experimental conditions.

The locales estimated using the C16/DAcPC partitioning (Figure 4) are in perfect agreement with the known locales for all compounds where this information is available (**1–4**, **6**, **10**, **12**, **15**, and **16**, Table 1). The difference between $\log P_{C16/W}$ and $\log P_{C16/O}$ values also perform well for these compounds, except compound **6**, which is predicted to reside in the headgroups, while the fluorescence quenching experiments located it at the interface.[21] The differences between the C16/DAcPC and C16/O systems are seen for compounds **5** – **9**: the C16/O prediction places them clearly into the headgroup region, while the C16/DAcPC prediction does not indicate a strong preference, except locating 3-bromoaniline (**5** in Table 1) in the core. As mentioned above, the locale for compound **6** is correctly predicted by the C16/DAcPC system. Unfortunately, no experimental data are available for compounds **5**, **7**, **8**, and **9**, to decide the contest at this point. Some insight can be obtained using observations on similar compounds.

Phenol is partitioning at the interface between the nonpolar regions and small aqueous regions inside inverted micelles in wet 1-octanol.[45] 4-*tert*-Octylphenol, having a chain of higher lipophilicity than the 4-Br substituent, interacts with the bilayer interface.[82] These facts indicate that 4-bromophenol (compound **7** in Table 1) more probably interacts with the interface than with the headgroups alone. A similar anticipation could be reached for 2-hydroxybiphenyl (compound **9** in Table 1) but the *ortho*-position of the hydroxy group complicates the situation. Aniline is a weaker H-bond donor than phenol.[83] Therefore, 3-bromoaniline (compound **5** in Table 1) is probably anchored less efficiently in the headgroup region than 4-bromophenol and

may partition in the core. In these cases, the C16/DAcPC system seems to be closer to the correct prediction than the C16/O system.

The solvation energies of a solute in C16 and in the hydrated DAcPC phase can be rationalized in terms of two contributions: the energies needed to form a cavity in either phase and the interactions of the solute molecule with the solvent molecules lining the cavity. The cavity formation energy is the highest in bulk water and decreases in the headgroup region to a minimum in the core.[22,70] A cavity in the isotropic DAcPC solution can probably be formed easier than in the headgroups because the headgroup anchoring effect of the high-density tail region 3 is missing in DAcPC. On the basis of these facts, we expect that the main contribution to the solvation energies in DAcPC and C16 comes from the interactions between the solutes and phospholipids. Thus, partitioning in the C16/DAcPC system is expected to provide only information about one of the factors contributing to the location in the bilayer, energy of interactions with the phospholipids. The cavity formation energy is a minor factor, and entropic factors as well as the energies of electrostatic interactions of the solutes with the membrane and dipole potentials are not included.

The solvation energies in the bilayer regions can be estimated using a correlation with the surrogate solvation energies in the C16/DAcPC system as was reported for many other solvent systems[26] and possibly with the estimates of the remaining three contributing factors. The refined solvation energies will provide a basis for a future system of fragment contributions for estimation of affinities of chemicals to individual bilayer regions. The planned approach has a potential to improve the knowledge and estimation of solvation energies of drugs and membrane-bound proteins in individual bilayer regions.

Acknowledgments

This work was supported in part by the NIH NCRR grants 1 P20 RR 15566 and 1 P20 RR 16471.

REFERENCES

1. Balaz S. Persp. Drug Discov. Design 2000;19:157–177.
2. Balaz S, Lukacova V. Quant. Struct. Act. Relat 1999;18:361–368.
3. Poulin P, Theil FP. J. Pharm. Sci 2002;91:129–156. [PubMed: 11782904]
4. Wang J, Schnell JR, Chou JJ. Biochem. Biophys. Res. Commun 2004;324:212–217. [PubMed: 15465004]
5. Ueda I, Yoshida T. Chem. Phys. Lipids 1999;101:65–79. [PubMed: 10810926]
6. White SH. FEBS Letters 2003;555:116–121. [PubMed: 14630330]
7. Goforth RL, Chi AK, Greathouse DV, Providence LL, Koeppe RE II, Andersen OS. J. Gen. Physiol 2003;121:477–493. [PubMed: 12719487]
8. Wiener MC, White SH. Biophys. J 1992;61:434–447. [PubMed: 1547331]
9. Marrink SJ, Berendsen HJC. J. Phys. Chem 1994;98:4155–4168.
10. Walter A, Gutknecht J. J. Membr. Biol 1986;90:207–217. [PubMed: 3735402]
11. Huster D, Jin AJ, Arnold K, Gawrisch K. Biophys. J 1997;73:855–864. [PubMed: 9251802]
12. Finkelstein A. J. Gen. Physiol 1976;68:127–135. [PubMed: 956767]
13. Subczynski WK, Hyde JS, Kusumi A. Biochemistry 1991;30:8578–8590. [PubMed: 1653601]
14. Subczynski WK, Lomnicka M, Hyde JS. Free Radical Res 1996;24:343–349. [PubMed: 8733938]
15. Walter A, Gutknecht J. J. Membr. Biol 1984;77:255–264. [PubMed: 6699907]
16. Moring J, Niego LA, Ganley LM, Trumbore MW, Herbette LG. Biophys. J 1994;67:2376–2386. [PubMed: 7696477]
17. Pebay PE, Dufourc EJ, Szabo AG. Biophys. Chem 1994;53:45–56. [PubMed: 7841331]
18. Henderson JM, Iannucci RM, Petersheim M. Biophys. J 1994;67:238–249. [PubMed: 7918992]

19. Okamura E, Nakahara M. J. Phys. Chem. B 1999;103:3505–3509.
20. Bartucci R, Mollica P, Sapia P, Sportelli L. Appl. Magn. Reson 1998;15:181–195.
21. Asuncion-Punzalan E, London E. Biochemistry 1995;34:11460–11466. [PubMed: 7547874]
22. Pohorille A, Wilson MA. J. Chem. Phys 1996;104:3760–3773. [PubMed: 11539401]
23. Bassolino-Klimas D, Alper HE, Stouch TR. J. Am. Chem. Soc 1995;117:4118–4129.
24. Repakova J, Capkova P, Vattulainen I, Holopainen JM. J. Phys. Chem. B 2004;108:13438–13448.
25. Hoff B, Strandberg E, Ulrich AS, Tieleman DP, Posten C. Biophys. J 2005;88:1818–1827. [PubMed: 15596514]
26. Collander R. Acta Chem. Scand 1951;5:774–780.
27. Hansch, C.; Leo, A. Substituent Constants for Correlation Analysis in Chemistry and Biology. New York: Wiley; 1979.
28. Giesen DJ, Hawkins GD, Liotard DA, Cramer CJ, Truhlar DG. Theor. Chem. Accounts 1997;98:85–109.
29. White SH, Ladokhin AS, Jayasinghe S, Hristova K. J. Biol. Chem 2001;276:32395–32398. [PubMed: 11432876]
30. Hansch, C.; Leo, A. Exploring QSAR: Fundamentals and Applications in Chemistry and Biology. Washington, DC: American Chemical Society; 1995.
31. Meyer H. Arch. Exp. Pathol. Pharmacol 1899;42:109–118.
32. Overton, E. Studien ueber die Narkose zugleich ein Betrag zur allgemeinen Pharmakologie. Jena: G. Fischer; 1901.
33. Bodansky M, Meigs AV. J. Phys. Chem 1932;36:814–818.
34. Tabern DL, Shelberg EF. J. Am. Chem. Soc 1933;55:328–332.
35. Macy R. J. Ind. Hyg. Toxicol 1948;30:140–143. [PubMed: 18905207]
36. Davies JT. J. Phys. Colloid Chem 1950;54:185–204.
37. Hansch C, Fujita T. J. Am. Chem. Soc 1964;86:1616–1626.
38. Margolis SA, Levenson M. Fresenius' J. Anal. Chem 2000;367:1–7. [PubMed: 11227426]
39. Jacobs RE, White SH. Biochemistry 1989;28:3421–3437. [PubMed: 2742845]
40. Wiener MC, King GI, White SH. Biophys. J 1991;60:568–576. [PubMed: 1932548]
41. Wimley WC, White SH. Nat. Struct. Biol 1996;3:842–848. [PubMed: 8836100]
42. Xiang T, Xu Y, Anderson BD. J. Membr. Biol 1998;165:77–90. [PubMed: 9705984]
43. Franks NP, Abraham MH, Lieb WR. J. Pharm. Sci 1993;82:466–470. [PubMed: 8360823]
44. Sassi P, Paolantoni M, Cataliotti RS, Palombo F, Morresi A. J. Phys. Chem. B 2004;108:19557–19565.
45. DeBolt SE, Kollman PA. J. Am. Chem. Soc 1995;117:5316–5340.
46. MacCallum JL, Tieleman DP. J. Am. Chem. Soc 2002;124:15085–15093. [PubMed: 12475354]
47. Ahmed M, Burton JS, Hadgraft J, Kellaway IW. J. Membr. Biol 1981;58:181–189. [PubMed: 7218338]
48. Dulfer WJ, Govers HAJ. Environ. Sci. Technol 1995;29:2548–2554.
49. De Young LR, Dill KA. J. Phys. Chem 1990;94:801–809.
50. Seydel, JK.; Wiese, M. Drug-Membrane Interactions: Analysis, Drug Distribution, Modeling. Weinheim: Wiley-VCH; 2003.
51. Osterberg T, Svensson M, Lundahl P. Eur. J. Pharm. Sci 2001;12:427–439. [PubMed: 11231109]
52. Fruttero R, Caron G, Fornatto E, Boschi D, Ermondi G, Gasco A, Carrupt PA, Testa B. Pharm. Res 1998;15:1407–1413. [PubMed: 9755893]
53. Gobas FAPC, Lahittete JM, Garofalo G, Shiu WY, Mackay D. J. Pharm. Sci 1988;77:265–272. [PubMed: 3373432]
54. Patel H, Schultz TW, Cronin MTD. THEOCHEM 2002;593:9–18.
55. Herbette LG, Chester DW, Rhodes DG. Biophys. J 1986;49:91–94. [PubMed: 19431663]
56. Balon K, Riebesehl BU, Müller BW. Pharm. Res 1999;16:882–888. [PubMed: 10397609]

57. Vaes WHJ, Ramos EU, Hamwijk C, van Holsteijn I, Blaauboer BJ, Seinen W, Verhaar HJM, Hermens JLM. Chem. Res. Toxicol 1997;10:1067–1072. [PubMed: 9348427]
58. Xiang TX, Chen X, Anderson BD. Biophys. J 1992;63:78–88. [PubMed: 1420875]
59. Xiang TX, Anderson BD. J. Pharm. Sci 1994;83:1511–1518. [PubMed: 7884677]
60. Mayer PT, Xiang TX, Anderson BD. PharmSci 2000;2 Article 14.
61. Davis, SS.; Higuchi, T.; Rytting, JH. Advances in Pharmaceutical Sciences. Bean, HS.; Beckett, AH.; Carless, JE., editors. Vol. Vol.4. London: Academic Press; 1974. p. 73-261.
62. Rekker, RF. The Hydrophobic Fragmental Constants: Its Derivation and Application. Amsterdam: Elsevier; 1977. p. 1-389.
63. Wiener MC, White SH. Biophys J 1992;61:428–433. [PubMed: 1547330]
64. Leahy DE, Taylor PJ, Wait AR. Quant. Struct. Act. Relat 1989;8:17–31.
65. Burton PS, Conradi RA, Hilgers AR, Ho NFH, Maggiora LL. J Control Release 1992;19:87–97.
66. Chiu SW, Clark M, Balaji V, Subramaniam S, Scott HL, Jakobsson E. Biophys. J 1995;69:1230–1245. [PubMed: 8534794]
67. Tieleman DP, Marrink SJ, Berendsen HJ. Biochim. Biophys. Acta 1997;1331:235–270. [PubMed: 9512654]
68. Xiang TX. J. Chem. Phys 1998;109:7876–7884.
69. Fischer H, Gottschlich R, Seelig A. J. Membr. Biol 1998;165:201–211. [PubMed: 9767674]
70. Pratt LR, Pohorille A. Chem. Rev 2002;102:2671–2692. [PubMed: 12175264]
71. Bemporad D, Luttmann C, Essex JW. Biophys. J 2004;87:1–13. [PubMed: 15240439]
72. Anderson RL, Davis S. Clin. Chim. Acta 1982;121:111–116. [PubMed: 6282500]
73. Origin. Northampton, MA: Microcal Software; 1999.
74. McIntosh TJ, Simon SA, Macdonald RC. Biochim. Biophys. Acta 1980;597:445–463. [PubMed: 6892885]
75. Gusev DG, Vasilenko IA, Evstigneeva RP. Biol. Membr 1986;3:685–690.
76. Okamura, E.; Nakahara, M. Liquid Interfaces in Chemical, Biological, and Pharmaceutical Applications. New York: Marcel Dekker; 2001. p. 775-805.
77. Barry JA, Gawrisch K. Biochemistry 1994;33:8082–8088. [PubMed: 8025114]
78. Okamura E, Kakitsubo R, Nakahara M. Langmuir 1999;15:8332–8335.
79. Seiler P. Eur. J. Med. Chem 1974;9:473–479.
80. Chikhale EG, Ng KY, Burton PS, Borchardt RT. Pharm. Res 1994;11:412–419. [PubMed: 8008709]
81. Caron G, Ermondi G. J. Med. Chem 2005;48:3269–3279. [PubMed: 15857133]
82. Kachel K, Asuncion-Punzalan E, London E. Biochemistry 1995;34:15475–15479. [PubMed: 7492549]
83. Reynisson J, Mcdonald E. J. Comput. Aid. Mol. Design 2004;18:421–431.

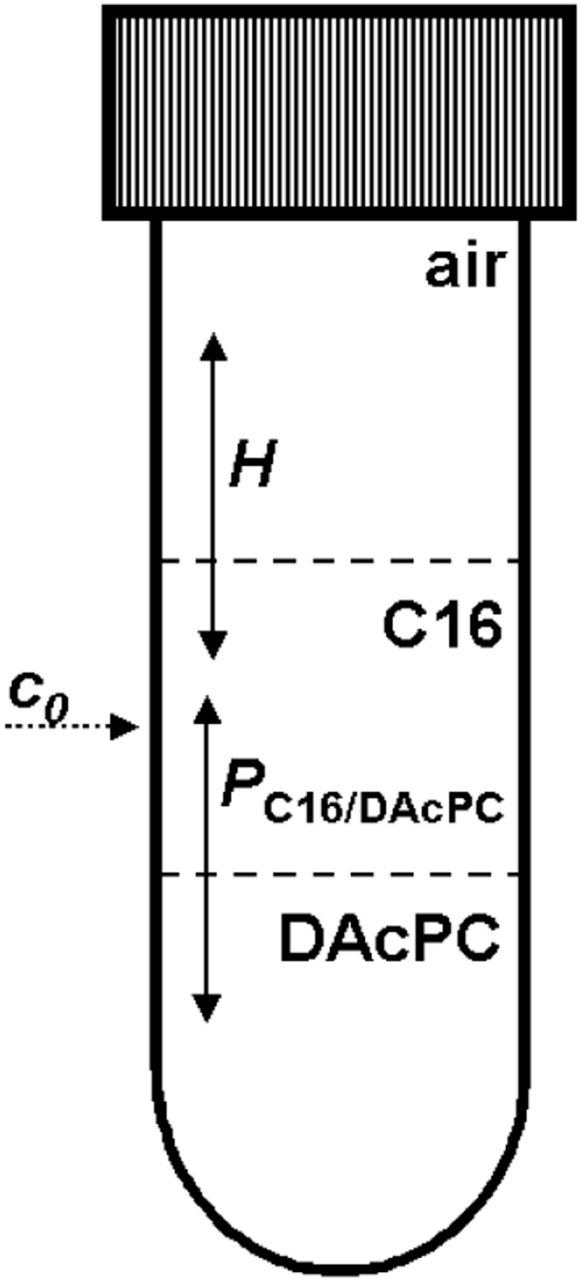

Figure 1.
A scheme for partitioning of organic compounds between air, C16 and hydrated DAcPC. For simplicity, the equilibrium constants are only shown: the partition coefficient *P* characterizing the partitioning equilibrium and the Henry constant *H* characterizing the evaporation equilibrium. The kinetics of evaporation and partitioning were analyzed using explicit solutions to the corresponding sets of linear differential equations.

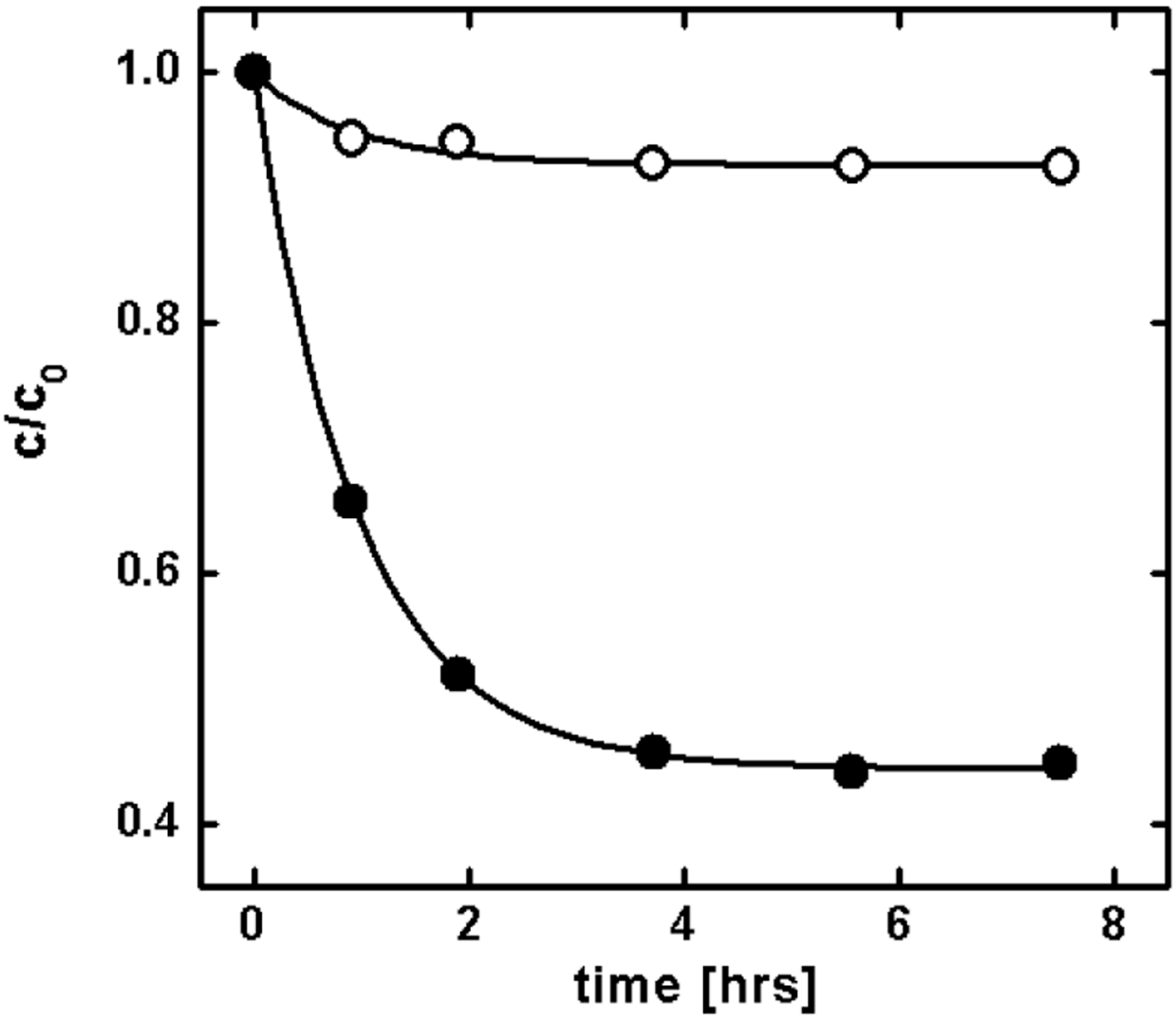

Figure 2.
Kinetics of partitioning of pyridine (**10**, Table 1) from C16 into the hydrated DAcPC phase. Solid points show the decrease of pyridine concentration in C16 caused by both partitioning and evaporation. Open points show evaporation of pyridine from control samples containing only pyridine in C16.

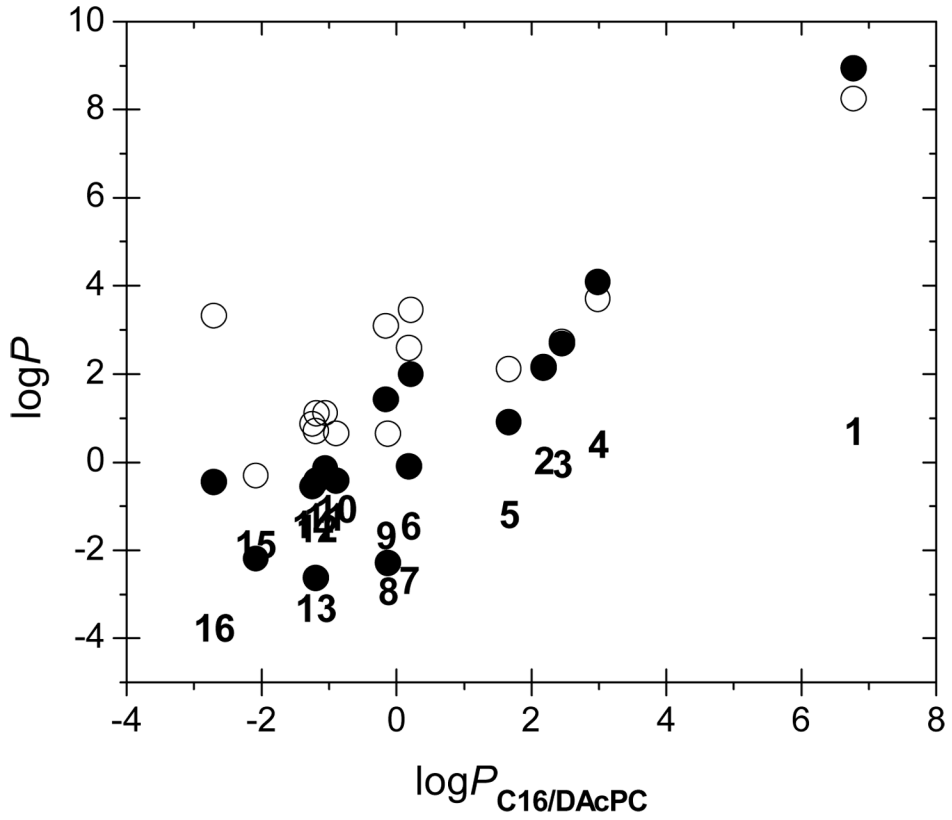

Figure 3.
The dependences between the partition coefficient in the C16/DAcPC system and the partition coefficients *P* in the systems C16/W (●), O/W (○), and C16/O (compound numbers, Table 1) that was obtained as $\log P_{C16/W} - \log P_{O/W}$.

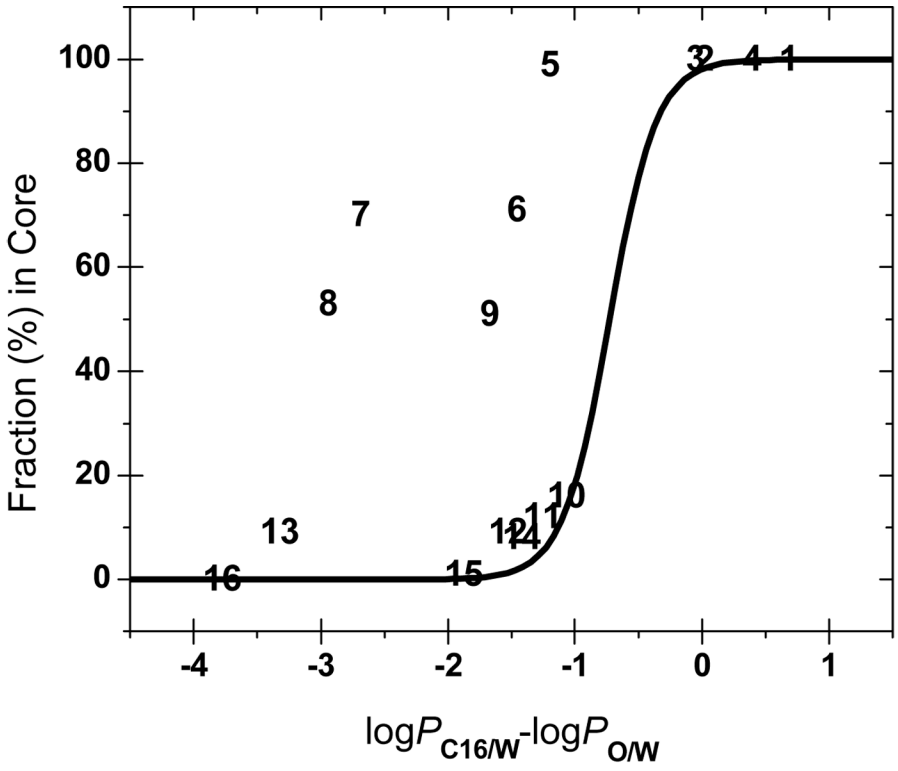

Figure 4.

Fraction in the core region as predicted from the C16/DAcPC partitioning as dependent on the C16/O partition coefficients. Experimentally, compounds **1–4** were located in the core, compound **6** at the interface, and compounds **10**, **12**, **15**, and **16** in the headgroups (Table 1). The sigmoidal curve connects the compounds with known locale in headgroups or the core and corresponds to Eq. 4.

Table 1

Partition Coefficients *P* and Distribution of Compounds in Bilayer

No.	Compound	log *P*			Fraction (%)[a]		Experiment	
		C16/DAcPC	C16/W	O/W	Core	Headgroups	Preferred Locale	Method
1	n-hexadecane	6.774 ± 0.354	8.93	8.25	100	0	core[74]	neutron diffraction
2	benzene	2.189 ± 0.076	2.15	2.13	100	0	core[75]; headgroups[76]	^{2}H and ^{31}P NMR; ^{1}H and ^{13}C NMR
3	toluene	2.454 ± 0.189	2.68	2.73	100	0	core[75]	^{2}H and ^{31}P NMR
4	n-propylbenzene	2.984[b]	4.08	3.69	100	0	core[19]	^{1}H and ^{13}C NMR shifts
5	3-bromoaniline	1.669 ± 0.022	0.90	2.10	99	1	N/A	-
6	9-anthracenemethanol	0.217 ± 0.067	1.99	3.45	71	29	interface[21]	fluorescence quenching
7	4-bromophenol	0.192 ± 0.084	−0.10	2.59	70	30	N/A	-
8	benzamide	−0.122 ± 0.068	−2.30	0.64	53	47	N/A	-
9	2-hydroxybiphenyl	−0.152 ± 0.044	1.42	3.09	51	49	N/A	-
10	pyridine	−0.885 ± 0.016	−0.42	0.65	16	84	headgroups[18]	^{2}H and ^{13}C MAS NMR
11	2,6-dimethoxyphenol	−1.054 ± 0.025	−0.15	1.11	12	88	N/A	-
12	benzylalcohol	−1.179 ± 0.011	−0.43	1.10	9	91	headgroups[19]	^{1}H and ^{13}C NMR shifts
13	4-amino-3-methylphenol	−1.186 ± 0.121	−2.63	0.697	9	91	N/A	-
14	2,3-diaminonaphthtalene	−1.694 ± 0.073	−0.56	0.862	3	97	N/A	-
15	ethanol	−2.081 ± 0.002	−2.19	−0.31	1	99	headgroups[77]	^{2}H and ^{31}P NMR
16	bisphenol A	−2.697 ± 0.100	−0.46	3.32	0	100	[c] headgroups[78]	^{1}H and ^{13}C NMR shifts

[a] Estimated using the $P_{C16/DAcPC}$ value and the headgroups:core volume ratio 2:3.

[b] Estimated using the fragment constant for methylene (= log *P* (**3**) − log *P* (**2**)) as log *P* (**3**) plus two methylene fragment values.[27]

[c] Bisphenol A interacts also with the first two CH_2 segments of the fatty acid chains.